PROCEEDINGS OF THE ROYAL SOCIETY A

FirstCite® e-publishing

Proc. R. Soc. A
doi:10.1098/rspa.2007.0382
Published online

Analytical solution for ground motion of a half space with a semi-cylindrical canyon and a beeline crack

By Gang Liu[1], Baohua Ji[1,*] and Diankui Liu[2]

[1]*Department of Engineering Mechanics, Tsinghua University, Beijing 100084, China*
[2]*School of Civil Engineering, Harbin Engineering University, Harbin 150001, China*

In earthquake engineering and strong motion seismology, an important issue is to describe and analyse the displacement amplitudes and the relative phases of motions of infrastructures on or nearby the ground surface. In this paper, the influence of a beeline crack on the ground motion of a half space with a semi-cylindrical canyon under anti-plane loading is studied. A novel method combining Green's function and complex functions that can consider very irregular topography is developed for deriving the function of ground motion of the half space. Analytical expressions for the displacement and stress in the half space are obtained. Our results show that the positions and dimensions of the canyon and the beeline crack have a big influence on the ground motion. The crack can amplify the amplitudes of the motion significantly, and its influence cannot be neglected until the distance between the crack and the ground reaches up to 100 times more than the dimension of the crack.

Keywords: ground motion, canyon; beeline crack; Green's function; complex function

1. Introduction

Seismic wave scattering by irregular topography is a very important and challenging problem in the field of earthquake engineering and strong motion seismology. During past decades, intensive studies were dedicated to understanding the mechanics of ground motion with irregular topography by theoretical and numerical approaches. For simple topography, e.g. a semi-cylindrical canyon (Trifunac 1973), a semi-elliptical canyon (Wong & Trifunac 1974) and a circular underground cavity (Lee 1977) or tunnel (Lee & Trifunac 1979), the analytical solutions for problems of anti-plane diffraction have been obtained. However, a more complex topography, e.g. the anti-plane diffraction from a canyon above a subsurface unlined tunnel with incident shear horizontal (SH) waves, was just pursued recently (Lee *et al.* 1999). The diffraction of a triangular dike on a flexible embedded foundation was studied by Todorovska *et al.* (2001) using a fractional order Bessel function. The problem of a

* Author for correspondence (bhji@mail.tsinghua.edu.cn).

Received 27 December 2007
Accepted 6 March 2008

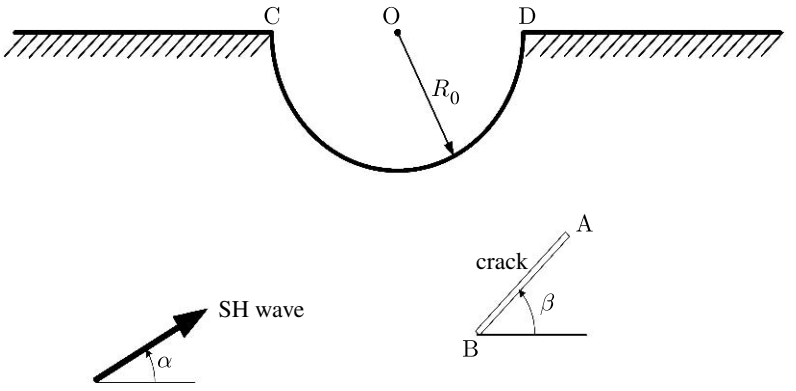

Figure 1. A half space with a semi-cylindrical canyon, a beeline crack and an incident SH wave coming from the left.

semi-circular hill above a subsurface cavity was studied using an advanced analytical method (Lee *et al.* 2006; Liu & Wang 2006). The above analytic solutions were obtained using the method of expansion of a wave function in polar coordinates, which can only deal with problems with relatively simple boundary conditions. If even more complex topography is considered, it will be very difficult for current approaches to obtain an analytic solution.

During the past 20 years, many numerical methods were successfully applied to solve the scattering problems caused by various irregular topographies or complex alluvium basins encountered in seismological studies. These methods include the boundary integral equation method (Aki & Richards 1980; Zhang & Chopra 1991) and the indirect boundary-element method (Yokoi & Sánchez-Sesma 1998). The semi-analytic methods include, but are not limited to, the Aki–Larner method (Aki & Larner 1970), the Bouchon–Campillo method (Campillo & Bouchon 1985; Bouchon 2003) and Chen's method (Chen 1999; Cao *et al.* 2004). Although the numerical methods are efficient for some complex engineering problems, the analytical method is essential to the understanding of the underlying physics of the problems. For analytical approaches, a big challenge is how to obtain the analytical solutions of elastic wave scattering under arbitrary boundary conditions and combined boundaries. A novel method, combining complex functions and multipolar coordinates, was recently developed by the authors and co-workers (Liu *et al.* 1982; Liu & Han 1991; Liu & Liu 2007), which can be applied to these problems. It is found that our method (Liu & Liu 2007) is effective in dealing with the problems with complex irregular topography. With complex functions, the wave functions can be conveniently transferred between different coordinates through the multipolar coordinates method without the *Graf* expansion (Lee *et al.* 1999) to handle the combined complicated boundaries.

In this work, we are interested in the anti-plane problem of scattering by a half space with a surface canyon and a beeline crack (figure 1). The crack is used to simulate a crack-like flaw below the basin. The existence of the crack and its interaction with the canyon should have a big influence on the ground motion of the half space. A critical challenge in this work is how to establish a wave function that is compatible with the intrinsic mechanics of the problem and satisfies all the

boundary conditions, especially to construct the traction-free conditions on crack surfaces. Here, a novel method simultaneously adopting Green's function, complex functions and multipolar coordinates will be developed and then applied to obtain analytical expressions of the displacement field of the surface.

2. Model and governing equations

For the anti-plane problem, the displacement satisfies the following Helmholtz equation:

$$\nabla^2 w = \frac{1}{c_s^2}\ddot{w}, \tag{2.1}$$

where $c_s = \sqrt{\mu/\rho}$ stands for the shear wave velocity; and ρ and μ are the mass density and shear modulus of elasticity of the media in the half space, respectively.

For the case of harmonic incident, the anti-plane displacement w can be set as $w = W(x_j)T(t)$. Separating the variables, (2.1) can be written in the polar coordinates

$$\frac{\partial^2 W}{\partial r^2} + \frac{1}{r}\frac{\partial W}{\partial r} + \frac{1}{r^2}\frac{\partial^2 W}{\partial \theta^2} + k^2 W = 0 \tag{2.2}$$

and

$$\ddot{T} + \omega^2 T = 0, \tag{2.3}$$

where $k = \omega/c_s$, ω is the circular frequency of the displacement, and the corresponding stress components are given by

$$\tau_{rz} = \mu\frac{\partial W}{\partial r} \tag{2.4}$$

and

$$\tau_{\theta z} = \frac{\mu}{r}\frac{\partial W}{\partial \theta}. \tag{2.5}$$

The solution of (2.3) is

$$T = \exp(\pm \mathrm{i}\omega t). \tag{2.6}$$

If we set $W = R(r)\Theta(\theta)$ in (2.2) and separate the variables, we can obtain

$$\frac{r^2}{R}\frac{\mathrm{d}^2 R}{\mathrm{d}r^2} + \frac{r}{R}\frac{\mathrm{d}R}{\mathrm{d}r} + k^2 r^2 = -\frac{1}{\Theta}\frac{\mathrm{d}^2\Theta}{\mathrm{d}\theta^2}. \tag{2.7}$$

Observing that the l.h.s. terms of the above equation are only functions of r and the r.h.s. term is only a function of θ, we set that they are both equal to a constant number $(mp)^2$, where m is an integer and p is a number determined by the boundary conditions. Then, we obtain

$$\frac{\mathrm{d}^2\Theta}{\mathrm{d}\theta^2} + (mp)^2\Theta = 0 \tag{2.8}$$

and

$$\frac{r^2}{R}\frac{\mathrm{d}^2 R}{\mathrm{d}r^2} + \frac{r}{R}\frac{\mathrm{d}R}{\mathrm{d}r} + k^2 r^2 - (mp)^2 = 0. \tag{2.9}$$

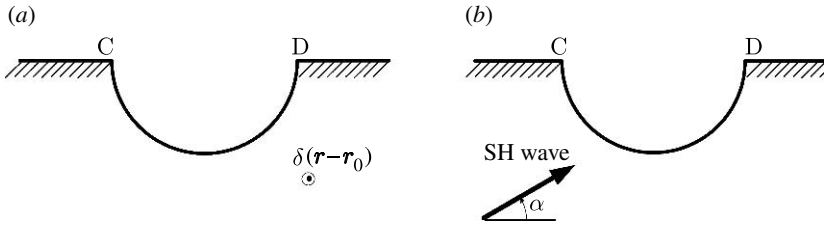

Figure 2. A half space with a semi-cylindrical canyon under (*a*) an anti-plane line source force and (*b*) incident SH waves.

The solution for (2.8) is

$$\Theta = \hbar \cos mp\theta + \lambda \sin mp\theta \quad \text{or} \quad \ell \mathrm{e}^{\pm \mathrm{i}mp\theta}. \tag{2.10}$$

We find that (2.9) is a Bessel equation with the order of mp and the variable is kr, so the solution of (2.9) is

$$R = J_{mp}(kr) \quad \text{or} \quad H_{mp}(kr), \tag{2.11}$$

where $J_{mp}(\cdot)$ is a Bessel function of order mp and $H_{mp}(\cdot)$ is a Hankel function of order mp. According to (2.6), (2.10) and (2.11), the solution of the governing equation (2.1) is obtained as (Liu & Liu 2007)

$$W = \sum_{m=-\infty}^{\infty} J_{mp}(kr)\mathrm{e}^{\pm \mathrm{i}mp\theta}\mathrm{e}^{\pm \mathrm{i}\omega t} \quad \text{or} \quad W = \sum_{m=-\infty}^{\infty} H_{mp}(kr)\mathrm{e}^{\pm \mathrm{i}mp\theta}\mathrm{e}^{\pm \mathrm{i}\omega t}. \tag{2.12}$$

When $|r| \to \infty$, the asymptotic expression of (2.12) is (Pao & Mow 1973)

$$W \to \sum_{m=-\infty}^{\infty} \sqrt{\frac{2}{\pi kr}} \cos\left(kr - \frac{m\pi}{2} - \frac{\pi}{4}\right) \mathrm{e}^{\pm \mathrm{i}mp\theta}\mathrm{e}^{\pm \mathrm{i}\omega t}$$

or

$$W \to \sum_{m=-\infty}^{\infty} \sqrt{\frac{2}{\pi kr}} \exp\left[\mathrm{i}\left(kr - \frac{m\pi}{2} - \frac{\pi}{4}\right)\right] \mathrm{e}^{\pm \mathrm{i}mp\theta}\mathrm{e}^{\pm \mathrm{i}\omega t}. \tag{2.13}$$

3. Green's function

Green's function of this problem is adopted as the displacement response of the elastic half space containing a semi-cylindrical canyon impacted by an anti-plane harmonic linear source force at a point in the half space (figure 2*a*). In a polar coordinate system, the governing equation of Green's function G is

$$\frac{\partial^2 G}{\partial r^2} + \frac{1}{r}\frac{\partial G}{\partial r} + \frac{1}{r^2}\frac{\partial^2 G}{\partial \theta^2} + k^2 G = \delta(\boldsymbol{r} - \boldsymbol{r}_0), \tag{3.1}$$

where $\boldsymbol{r}_0$ stands for the position of the linear source force in polar coordinates, $\boldsymbol{r}_0 = r_0 \exp(\mathrm{i}\theta_0)$, and $\boldsymbol{r}$ stands for the position of the observation point, $\boldsymbol{r} = r \exp(\mathrm{i}\theta)$. The boundary conditions can be expressed as

$$\tau_{rz} = 0 \quad \text{at} \quad r = R_0 \tag{3.2}$$

and

$$\tau_{\theta z} = 0 \quad \text{at} \quad \theta = 0, \pi. \tag{3.3}$$

The basic solution that satisfies the control equation (3.1) and the boundary conditions (3.2) and (3.3) should include two parts of the motion, the disturbance of the anti-plane linear source force and the scattering wave induced by the semi-cylindrical canyon. The response of the half space due to the line source load $\delta(\boldsymbol{r}-\boldsymbol{r}_0)$ is given by

$$G^{(i)} = \frac{\mathrm{i}}{4\mu} H_0^{(1)}(k|\boldsymbol{r}-\boldsymbol{r}_0|), \tag{3.4}$$

where $H_0^{(1)}(\cdot)$ is the first kind of the *Hankel* function with zero order. According to the addition theorem of the Bessel function, (3.4) can be written as (Pao & Mow 1973)

$$G^{(i)} = \frac{\mathrm{i}}{4\mu} \sum_{m=0}^{\infty} \varepsilon_m \cos\big[m(\theta-\theta_0)\big] \begin{cases} J_m(kr_0)H_m^{(1)}(kr), & r > r_0, \\ J_m(kr)H_m^{(1)}(kr_0), & r < r_0, \end{cases} \tag{3.5}$$

when $m=0$, $\varepsilon_m=1$; $m\geq 1$, $\varepsilon_m=2$.

According to the 'symmetry theory' (Lee *et al.* 1999), the wave reflected by a horizontal surface can be written as

$$G^{(r)} = \frac{\mathrm{i}}{4\mu} H_0^{(1)}(k|\boldsymbol{r}-\bar{\boldsymbol{r}}_0|), \tag{3.6}$$

where $\bar{\boldsymbol{r}}_0$ stands for the conjugate of $\boldsymbol{r}_0$ where the linear source force is applied in polar coordinates and $\bar{\boldsymbol{r}}_0 = r_0 \exp(-\mathrm{i}\theta_0)$. According to the addition theorem of the Bessel function, (3.6) can be written as

$$G^{(r)} = \frac{\mathrm{i}}{4\mu} \sum_{m=0}^{\infty} \varepsilon_m \cos\left[m(\theta+\theta_0)\right] \begin{cases} J_m(kr_0)H_m^{(1)}(kr), & r > r_0, \\ J_m(kr)H_m^{(1)}(kr_0), & r < r_0. \end{cases} \tag{3.7}$$

The scattering wave induced by the semi-cylindrical canyon can be written as

$$G^{(is)} = \sum_{m=0}^{\infty} A_m \cos\left[m(\theta-\theta_0)\right] H_m^{(1)}(kr) \tag{3.8}$$

and

$$G^{(rs)} = \sum_{m=0}^{\infty} B_m \cos\left[m(\theta+\theta_0)\right] H_m^{(1)}(kr), \tag{3.9}$$

where A_m and B_m are unknown coefficients. Therefore, the total wave function is

$$G = G^{(i)} + G^{(r)} + G^{(is)} + G^{(rs)}. \tag{3.10}$$

In order to satisfy the stress-free condition on the surface of the semi-cylindrical canyon, the total wave function G must satisfy the following equation:

$$\mu \frac{\partial G}{\partial r}\bigg|_{r=R_0} = 0. \tag{3.11}$$

Substituting (3.5), (3.7), (3.8) and (3.9) into (3.11) and considering $R_0 < r_0$, (3.11) can be transformed into

$$\begin{aligned}\frac{\mathrm{i}}{4\mu}\sum_{m=0}^{\infty}\varepsilon_m \cos\left[m(\theta-\theta_0)\right]J_m'(kR_0)H_m^{(1)}(kr_0)\\ +\frac{\mathrm{i}}{4\mu}\sum_{m=0}^{\infty}\varepsilon_m \cos\left[m(\theta+\theta_0)\right]J_m'(kR_0)H_m^{(1)}(kr_0)\\ +\sum_{m=0}^{\infty}A_m \cos\left[m(\theta-\theta_0)\right]H_m^{(1)\prime}(kR_0)\\ +\sum_{m=0}^{\infty}B_m \cos\left[m(\theta+\theta_0)\right]H_m^{(1)\prime}(kR_0)=0. \end{aligned} \tag{3.12}$$

The total displacement should satisfy the traction-free condition on the surface (at $y=0$). Setting $A_m = B_m$, the unknown coefficients A_m and B_m in (3.12) can be obtained as

$$A_m = -\frac{\mathrm{i}}{4\mu}\varepsilon_m \frac{J_m'(kR_0)H_m^{(1)}(kr_0)}{H_m^{(1)\prime}(kR_0)} \tag{3.13}$$

and

$$B_m = -\frac{\mathrm{i}}{4\mu}\varepsilon_m \frac{J_m'(kR_0)H_m^{(1)}(kr_0)}{H_m^{(1)\prime}(kR_0)}, \tag{3.14}$$

where $J_m'(\cdot)$ is the derivative of $J_m(\cdot)$ and $H_m^{(1)\prime}(\cdot)$ is the derivative of $H_m^{(1)}(\cdot)$. Substituting (3.13) and (3.14) into (3.8) and (3.9), respectively, and then substituting (3.5), (3.7), (3.8) and (3.9) into (3.10), the total wave function G can be obtained as

$$\begin{aligned}G(r,r_0,\theta,\theta_0) =& \frac{\mathrm{i}}{4\mu}\sum_{m=0}^{\infty}\varepsilon_m\{\cos\left[m(\theta-\theta_0)\right]+\cos\left[m(\theta+\theta_0)\right]\}J_m(kr)H_m^{(1)}(kr_0)\\ &-\sum_{m=0}^{\infty}\frac{\mathrm{i}}{2\mu}\varepsilon_m \cos m\theta \cos m\theta_0 \frac{J_m'(kR_0)H_m^{(1)}(kr_0)}{H_m^{(1)\prime}(kR_0)}H_m^{(1)}(kr). \end{aligned} \tag{3.15}$$

Applying the addition theorem of the Bessel function reversely, (3.15) can be transformed into

$$\begin{aligned}G(r,r_0,\theta,\theta_0) =& \frac{\mathrm{i}}{4\mu}\left\{\left[H_0^{(1)}(k|\boldsymbol{r}-\boldsymbol{r}_0|)+H_0^{(1)}(k|\boldsymbol{r}-\bar{r}_0|)\right]\right.\\ &\left.-\sum_{m=0}^{\infty}2\varepsilon_m \cos m\theta \cos m\theta_0 \frac{J_m'(kR_0)H_m^{(1)}(kr_0)}{H_m^{(1)\prime}(kR_0)}H_m^{(1)}(kr)\right\}. \end{aligned} \tag{3.16}$$

4. Scattering by a half space with a semi-cylindrical canyon

First, we consider the incidence of an SH wave on the linear elastic half space containing a semi-cylindrical canyon (Trifunac 1973), and the model is as shown in figure 2*b*. The harmonic incident displacement field $W^{(i)}$ can be written as follows:

$$W^{(i)} = W_0 \exp[\mathrm{i}kr\cos(\theta-\alpha)] = W_0 \sum_{n=0}^{\infty} \varepsilon_n i^n \cos[n(\theta-\alpha)] J_n(kr), \tag{4.1}$$

which is the expansion with wavevector kr that forms an angle α with the x-axis, where α is the incident angle and $k=\omega/c_s$ is the shear wavenumber of the media. If $n=0$, $\varepsilon_n=1$ then $n\geq 1$, $\varepsilon_n=2$. The wave reflected by the horizontal surface can be written as

$$W^{(r)} = W_0 \exp[\mathrm{i}kr\cos(\theta+\alpha)] = W_0 \sum_{n=0}^{\infty} \varepsilon_n i^n \cos[n(\theta+\alpha)] J_n(kr). \tag{4.2}$$

The scattering wave induced by the semi-cylindrical canyon is

$$W^{(is)} = W_0 \sum_{n=0}^{\infty} A_n H_n^{(1)}(kr)\cos[n(\theta-\alpha)] \tag{4.3}$$

and

$$W^{(rs)} = W_0 \sum_{n=0}^{\infty} B_n H_n^{(1)}(kr)\cos[n(\theta+\alpha)], \tag{4.4}$$

where A_n and B_n are unknown coefficients. Using the stress-free condition on the surface of the semi-cylindrical canyon, we have

$$\mu \frac{\partial\left(W^{(i)} + W^{(r)} + W^{(is)} + W^{(rs)}\right)}{\partial r}\bigg|_{r=R_0} = 0. \tag{4.5}$$

This total displacement should satisfy the traction-free condition on the surface (at $y=0$). Setting $A_n=B_n$, we can get the coefficients A_n and B_n as

$$A_n = -\varepsilon_n i^n \frac{J_n'(kR_0)}{H_n^{(1)\prime}(kR_0)} \tag{4.6}$$

and

$$B_n = -\varepsilon_n i^n \frac{J_n'(kR_0)}{H_n^{(1)\prime}(kR_0)}. \tag{4.7}$$

Therefore, the total wave field is obtained as

$$\begin{aligned} W &= W^{(i)} + W^{(r)} + W^{(is)} + W^{(rs)} \\ &= 2W_0 \sum_{n=0}^{\infty} \varepsilon_n i^n \left[J_n(kr) - \frac{J_n'(kR_0)}{H_n^{(1)\prime}(kR_0)} H_n^{(1)}(kr) \right] \cos n\theta \cos n\alpha. \end{aligned} \tag{4.8}$$

The corresponding stresses are given by

$$\tau_{rz} = 2\mu W_0 k \sum_{n=0}^{\infty} \varepsilon_n i^n \left[J_n'(kr) - \frac{J_n'(kR_0)}{H_n^{(1)'}(kR_0)} H_n^{(1)'}(kr) \right] \cos n\theta \cos n\alpha \tag{4.9}$$

and

$$\tau_{\theta z} = \frac{-2\mu W_0}{r} \sum_{n=0}^{\infty} n\varepsilon_n i^n \left[J_n(kr) - \frac{J_n'(kR_0)}{H_n^{(1)'}(kR_0)} H_n^{(1)}(kr) \right] \sin n\theta \cos n\alpha. \tag{4.10}$$

5. Wave functions and the stress field in new coordinates

By introducing the complex plane, $z = x + y\mathrm{i}$ and $\bar{z} = x - y\mathrm{i}$, the wave functions (3.16) and (4.8) are converted into

$$G(z, z_0) = \frac{\mathrm{i}}{4\mu} \left\{ \left[H_0^{(1)}(k|z - z_0|) + H_0^{(1)}(k|z - \bar{z}_0|) \right] - \sum_{m=0}^{\infty} 2\varepsilon_m \cos m\theta \cos m\theta_0 \frac{J_m'(kR_0)}{H_m^{(1)'}(kR_0)} H_m^{(1)}(k|z_0|) H_m^{(1)}(k|z|) \right\} \tag{5.1}$$

and

$$W = 2W_0 \sum_{n=0}^{\infty} \varepsilon_n i^n \left[J_n(k|z|) - \frac{J_n'(kR_0)}{H_n^{(1)'}(kR_0)} H_n^{(1)}(k|z|) \right] \cos n\theta \cos n\alpha. \tag{5.2}$$

In order to express the traction-free condition conveniently on the surface of the crack, we introduce new coordinates (x', y') and the corresponding new complex plane $(z', \bar{z}')$ by rotating the original coordinates (x, y), where $z' = x' + y'\mathrm{i}$, $\bar{z}' = x' - y'\mathrm{i}$, $z = z'\mathrm{e}^{\mathrm{i}\beta}$, $\bar{z} = \bar{z}'\mathrm{e}^{-\mathrm{i}\beta}$ and β is the inclined angle of the crack. In the new complex plane $(z', \bar{z}')$, the expressions of wave functions (5.1) and (5.2) are changed into

$$G(z', z_0') = \frac{\mathrm{i}}{4\mu} \left\{ \left[H_0^{(1)}\left(k|z'\mathrm{e}^{\mathrm{i}\beta} - z_0'\mathrm{e}^{\mathrm{i}\beta}|\right) + H_0^{(1)}\left(k|z'\mathrm{e}^{\mathrm{i}\beta} - \bar{z}_0'\mathrm{e}^{-\mathrm{i}\beta}|\right) \right] - \sum_{m=0}^{\infty} 2\varepsilon_m \cos m(\theta' + \beta) \cos m\left(\theta_0' + \beta\right) \frac{J_m'(kR_0)}{H_m^{(1)'}(kR_0)} \times H_m^{(1)}\left(k|z_0'|\right) H_m^{(1)}(k|z'|) \right\} \tag{5.3}$$

and

$$W = 2W_0 \sum_{n=0}^{\infty} \varepsilon_n i^n \left[J_n(k|z'|) - \frac{J_n'(kR_0)}{H_n^{(1)'}(kR_0)} H_n^{(1)}(k|z'|) \right] \times \cos n(\theta' + \beta) \cos n(\alpha' + \beta). \tag{5.4}$$

where z_0' is the position of the linear source force in the complex plane $(z', \bar{z}')$, $\bar{z}_0'$ is the conjugate of z_0' and α' stands for the incident angle in the new complex plane $(z', \bar{z}')$.

The stress fields induced by the wave function (5.4) in the new coordinates $(z', \bar{z}')$ are

$$\begin{aligned}\tau_{x'z} = \mu\frac{\partial W}{\partial x'} &= 2\mu W_0 k\sum_{n=0}^{\infty}\varepsilon_n i^n \cos\, n(\theta'+\beta)\cos\, n(\alpha'+\beta)\\ &\quad\times\left[J_n'(k|z'|) - \frac{J_n'(kR_0)}{H_n^{(1)'}(kR_0)}H_n^{(1)'}(k|z'|)\right]\frac{x'}{|z'|}\\ &\quad+2\mu W_0\sum_{n=0}^{\infty}\varepsilon_n i^n n\sin n(\theta'+\beta)\cos\, n(\alpha'+\beta)\\ &\quad\times\left[J_n(k|z'|) - \frac{J_n'(kR_0)}{H_n^{(1)'}(kR_0)}H_n^{(1)}(k|z'|)\right]\frac{y'}{|z'|^2}\end{aligned} \tag{5.5}$$

and

$$\begin{aligned}\tau_{y'z} = \mu\frac{\partial W}{\partial y'} &= 2\mu W_0 k\sum_{n=0}^{\infty}\varepsilon_n i^n \cos\, n(\theta'+\beta)\,\cos\, n(\alpha'+\beta)\\ &\quad\times\left[J_n'(k|z'|) - \frac{J_n'(kR_0)}{H_n^{(1)'}(kR_0)}H_n^{(1)'}(k|z'|)\right]\frac{y'}{|z'|}\\ &\quad-2\mu W_0\sum_{n=0}^{\infty}\varepsilon_n i^n n\sin n(\theta'+\beta)\,\cos n(\alpha'+\beta)\\ &\quad\times\left[J_n(k|z'|) - \frac{J_n'(kR_0)}{H_n^{(1)'}(kR_0)}H_n^{(1)}(k|z'|)\right]\frac{x'}{|z'|^2}.\end{aligned} \tag{5.6}$$

6. Scattering by the half space with both a semi-cylindrical canyon and a crack

Now, we consider the scattering of the incident SH wave when the semi-cylindrical canyon and crack coexist in the half space. Based on the incident and scattering fields of the half space containing only a semi-cylindrical canyon and Green's function of the half space containing the semi-cylindrical canyon with a harmonic anti-plane line source force we derived in previous sections, we can construct the wave function of scattering by a half space containing both the semi-cylindrical canyon and the beeline crack.

According to the solution of the scattering of the SH wave by the half space with only the semi-cylindrical canyon, we can calculate the stress value on a line AB where the crack will be constructed. Then, opposite anti-plane stresses of exactly the same magnitude $-\tau_{y'z}$ are loaded at the same position as AB, which induces a zero resultant force on AB (i.e. traction free), so that AB is equivalent to a crack, as shown in figure 3.

The additional displacement field induced by $-\tau_{y'z}$ can be obtained as

$$-\tau_{y'z}G\big(z', z_0'\big). \tag{6.1}$$

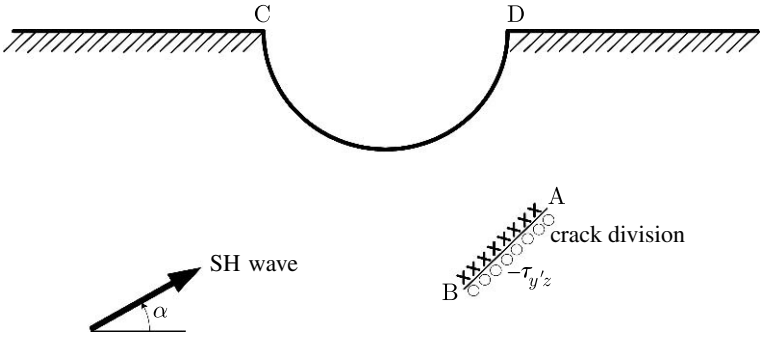

Figure 3. Illustration of constructing a subsurface crack using Green's function.

Integrating along the line of crack AB, we can obtain

$$-\int_{x_1'}^{x_2'} \tau_{y'z} G\left(z', z_0'\right) \mathrm{d}x'. \tag{6.2}$$

Hence, the total displacement field can be written as

$$W^{(t)} = W - \int_{x_1'}^{x_2'} \tau_{y'z} G\left(z', z_0'\right) \mathrm{d}x', \tag{6.3}$$

where W, $\tau_{y'z}$ and $G(z', z_0')$ are shown in (5.4), (5.6) and (5.3), respectively, and x_1' and x_2' stand for the positions of the points A and B, respectively, of the crack in coordinates (x', y').

The dimensionless parameters used in this paper are defined as follows: x/R_0 is the non-dimensional x coordinate normalized by the radius of the canyon R_0; $2R_0/b$ is the ratio of the radius of the canyon to the dimension of the beeline crack; $2a/b$ is the ratio of the distance between the crack and the horizontal surface to the dimension of the crack; and η is defined as $\eta = kR_0 = \omega R_0/c_s = 2R_0\pi/\lambda$ for convenience of discussion of the influence of the crack size on the surface motion, where kR_0 is the dimensionless wavenumber (we assume $R_0 = 1$). It also represents a dimensionless frequency $\omega R_0/c_s$, as well as 2π times the ratio of the radius of the canyon to the wavelength λ of the waves. The ground motion is characterized by the amplitudes of the total motion $|W/W_0|$. For convenience of discussion in the following, we assume that the crack is located directly below the canyon, and the incident plane SH waves come from the left, as shown in figure 4.

7. Results and discussions

With the novel method developed in this work, we can study the influence of the crack on the ground motion of the half space. All the calculations are performed with a MATLAB code. In order to check the validity of our new method, we calculate the ground motion of a half space with only the semi-cylindrical canyon. That is, we set the length of the crack to $b = 0$. This condition corresponds to the case of a half space with the canyon without the crack. Figure 5 illustrates the amplitude of the surface motion with $\eta = 1.0$ and $\alpha = 60°$

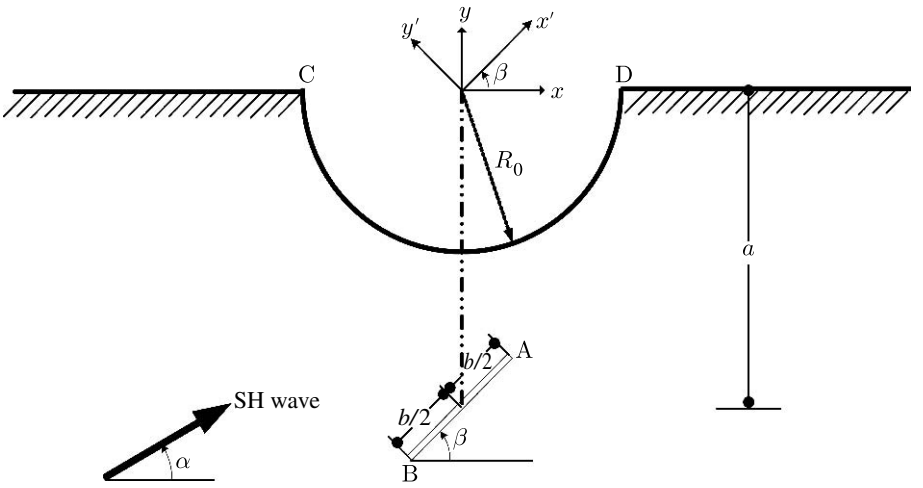

Figure 4. Illustration of the model of a half space with a semi-cylindrical canyon and beeline crack, where the crack is directly below the centre of the canyon.

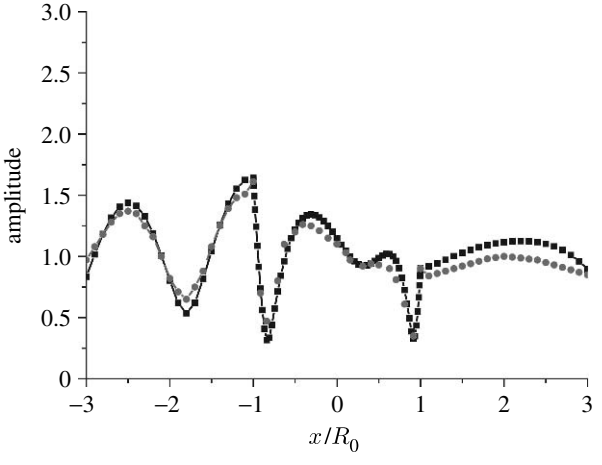

Figure 5. Our results (squares) in comparison with those of Zhou & Chen (2006; circles).

(this angle value corresponds to $\theta = 30°$ in the work of Zhou & Chen 2006). It can be seen that the analytical results are consistent with the numerical results of Zhou & Chen (2006) of the scattering by a half space with a semi-cylindrical canyon, except at the two rims (points C and D), i.e. $x/R_0 = \pm 1$. Our results show that the amplitude of the surface motion is a continuum at the rims of $x/R_0 = \pm 1$, but Zhou & Chen's results show that the amplitude at the two rims is discontinuous. More results with various incident angles, $\alpha = 0°$, 30°, 60° and 90°, and incident wavenumbers $\eta = 0.1$, 1.0, 1.5 and 2.5, are shown in figure 6*a* for comparison with those when the crack is present.

To study the influence of an existing crack on the ground motion, we set the distance between the semi-cylindrical canyon and the centre of the crack to $a = 2.5$, the length of the crack to $b = 2$ and the oblique angle of the beeline crack to

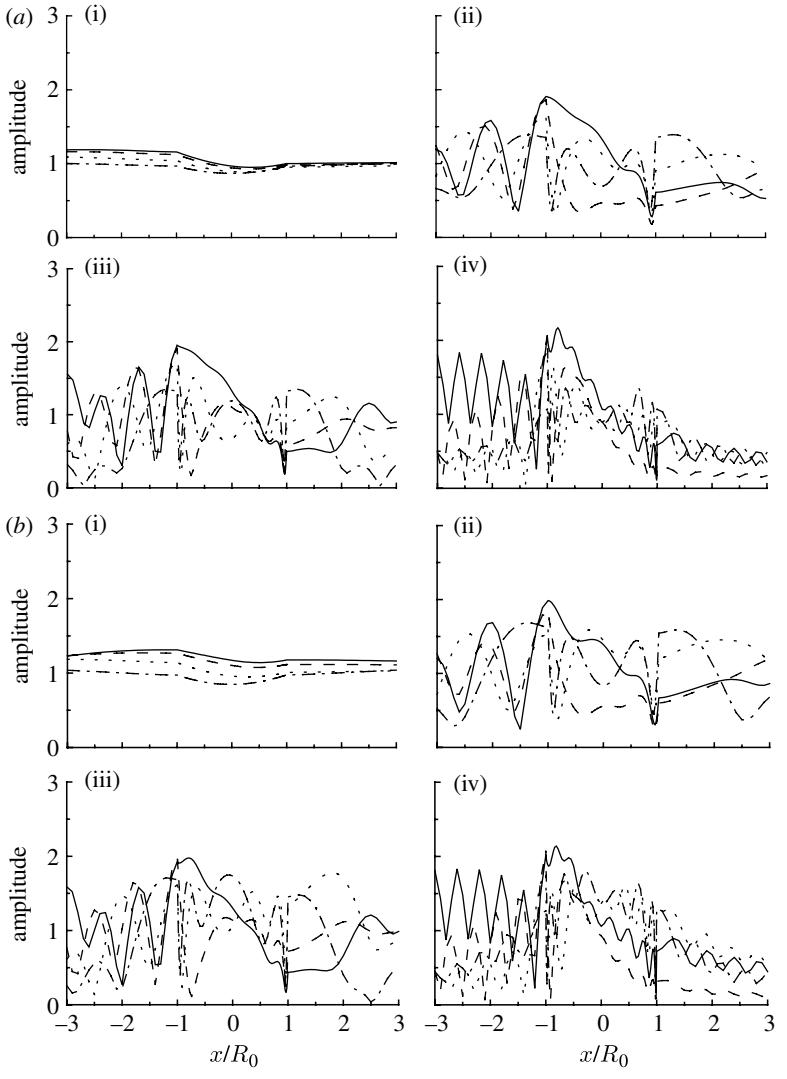

Figure 6. (a(i)–(iv)) Amplitudes of the ground motion without a crack; (b(i)–(iv)) amplitudes of the ground motion with a subsurface crack, where $b=2$ and $\beta=45°$ ((i) $\eta=0.1$ (solid line, $\alpha=0°$; dashed line, 30°; dotted line, 60°; dashed dotted line, 90°), (ii) $\eta=1.0$, (iii) $\eta=1.5$ and (iv) $\eta=2.5$).

$\beta=45°$. Figure 6b shows the amplitude of the surface motion with the presence of the crack. In comparison with the no-crack condition (as shown in figure 6a), we find that the crack amplifies the amplitudes of the surface motion both left and right of the canyon, especially at low frequency ($\eta=0.1$). However, at high frequencies, the amplitudes of the l.h.s. ($x/R_0\leq -1$) keep almost the same magnitude as those without the crack. By contrast, the amplitudes of the r.h.s. ($x/R_0\geq -1$) are amplified distinctly. These general characters of surface motion result from the scattering and diffraction of SH waves by the semi-cylindrical canyon and subsurface crack, as well as a decrease of the stiffness of the global structure due to the existence of the crack. Previous studies (Lee *et al.* 1999) have shown that a subsurface unlined tunnel under the semi-cylindrical canyon plays similar roles to the crack.

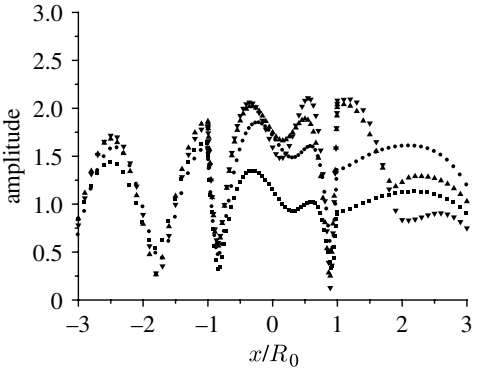

Figure 7. Amplitudes of the ground motion for different sizes of the beeline crack (squares, $b=0$; circles, $b=2$, $a=2$; up triangles, $b=4$, $a=2$; down triangles, $b=5$, $a=2$).

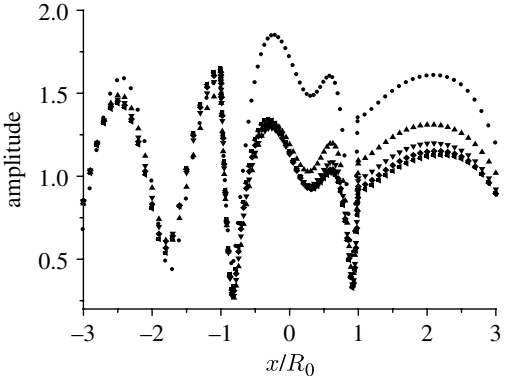

Figure 8. Amplitudes of the ground motion for different positions of the beeline crack (squares, $b=0$; circles, $b=2$, $a=2$; up triangles, $b=2$, $a=6$; down triangles, $b=2$, $a=10$; left triangles, $b=2$, $a=200$; diamonds, $b=2$, $a=20$).

Now, we study the effect of the size and position of the crack on the ground motion. We set the slantwise angle of the crack to $\beta=45°$, incident angle to $\alpha=60°$ and frequency of the incident wave to $\eta=1.0$. Figure 7 illustrates the ground motion amplitude versus the size of the crack (length of crack $b=2$, 4 and 5, respectively). The numerical results show that the displacement amplitudes are obviously amplified as the crack size increases, especially in the region at the r.h.s. of the rim C. Figure 8 shows that the position of the crack can have a significant effect on the ground motion amplitude. If we continuously increase the distance between the centre of the crack and the origin ($a=2$, 6, 10, 20, …, 200), the amplitudes of ground motion will decrease until this distance reaches up to 100 times larger than the size of the crack. The system at this limiting condition ($b=2$ and $a=200$) is equivalent to a half space containing a semi-cylindrical canyon, but without a crack. The decay of the influence of the beeline crack is slow because the anti-plane motion around the crack decreases at the rate of $x^{-1/2}$, which is slower than the rate of $x^{-3/2}$ in the in-plane motion.

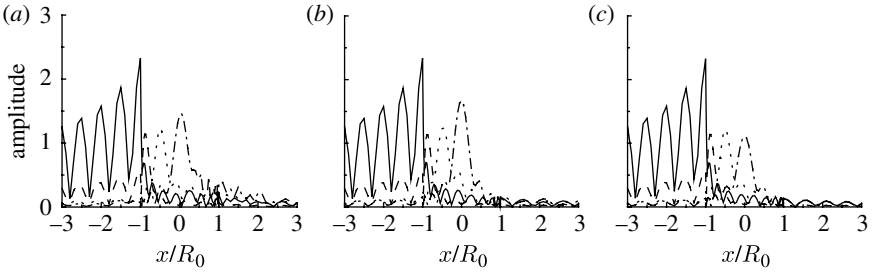

Figure 9. Amplitudes of the ground motion at different slantwise angles of crack with $\eta=12.0$, $2a/b=2.5$, $2R_0/b=1.0$, where (*a*) $\beta=0°$, (*b*) $\beta=45°$ and (*c*) $\beta=90°$ (solid line, $\alpha=0°$; dashed line, 30°; dotted line, 60°; dashed dotted line, 90°).

Figure 9 shows the amplitudes of motion at a very high frequency $\eta=12$, and at various incident angles $\alpha=0°$, 30°, 60° and 90°, with the slantwise angles of the crack being $\beta=0°$, 45° and 90° (as shown in figure 9*a–c*). Consistent with previous work (Lee *et al.* 1999), the amplitudes of motion at the front of the canyon are in general more complex and larger than those at the back. It should be noted that the maximum amplitude (equal to 2.34) occurs at the left rim C when $\alpha=0°$ and $\beta=45°$. As can be seen, at a specific position of the crack, the slantwise angle of the beeline crack does not affect the amplitudes significantly under high frequency incidence, except for $\alpha=90°$. When the crack is parallel with the incident wave, i.e. a vertical crack ($\beta=90°$) with vertical incidence ($\alpha=90°$), or a horizontal crack ($\beta=0°$) with horizontal incidence ($\alpha=0°$), the amplitudes of the ground motion exhibit almost the same characters as those of the half space without the crack. We call this phenomenon 'sweep incidence'. We note that the amplitudes of the motion tend to be smoother at the r.h.s. of the canyon, which may be attributed to energy absorption and resistance of propagation of the incident waves by the semi-cylindrical canyon at this frequency. This suggests that it might be possible to carve artificial caves to protect important structures behind them from the dynamic impact of certain frequencies.

Figure 10 is a three-dimensional plot of the amplitudes of ground motion at different radii of the semi-cylindrical canyon with a horizontal crack of constant size ($b=2$) under incident SH waves (figure 10*a*,*b* corresponds to $2a/b=2.5$, $2R_0/b=1.0$, at $\alpha=0°$ and 45°, respectively, and figure 10*c*,*d* corresponds to $2a/b=2.5$, $2R_0/b=0.25$, at $\alpha=0°$ and 45°, respectively). Here, we define a new dimensionless frequency $f=b\pi/\lambda$ in order to study the effect of the radius of the canyon on the ground motion. For horizontal incidence (as shown in figure 10*a*,*c*), we find that the amplitudes of the ground motion are complex on the l.h.s. of the canyon ($x/R_0\leq 0$), and the amplitudes decrease and become smoother on the r.h.s. ($x/R_0\geq 0$). The maximum amplitudes occur at the points around $x/R_0=-1$, $|W/W_0|=2.76$ (figure 10*a*) and $x/R_0=-1.1$, $|W/W_0|=1.90$ (figure 10*c*). The maximum values occur at these positions because the diffraction waves are excited around the tip of the canyon, which results in the amplification of the motion. Again, it is shown that the amplitudes tend to be smoother on the r.h.s. of the canyon. For oblique incidence (i.e. $\alpha=45°$ as shown in figure 10*b*,*d*), the displacement amplitudes increase with frequency on both sides of the surface at low frequency, but decreases after it reaches its maximum

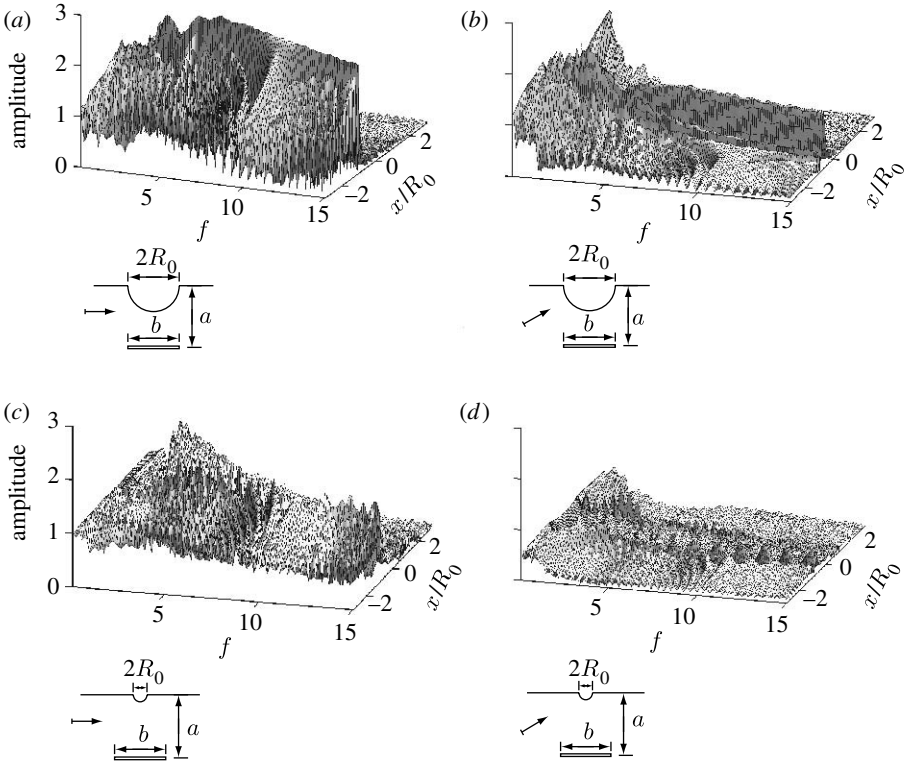

Figure 10. Three-dimensional plots of amplitudes of the ground motion with $0 \leq f \leq 15.0$. (*a*) $2a/b=2.5$, $2R_0/b=1.0$, at $\alpha=0°$ ($|W/W_0|=2.76$ at $\eta=6.6$, $x/R_0=-1$); (*b*) $2a/b=2.5$, $2R_0/b=1.0$, at $\alpha=45°$ ($|W/W_0|=2.05$ at $\eta=2.7$, $x/R_0=-1$); (*c*) $2a/b=2.5$, $2R_0/b=0.25$, at $\alpha=0°$ ($|W/W_0|=1.90$ at $\eta=4.8$, $x/R_0=-1.1$); (*d*) $2a/b=2.5$, $2R_0/b=0.25$, at $\alpha=45°$ ($|W/W_0|=1.77$ at $f=2.4$, $x/R_0=1.3$).

value, and the maximum amplitudes occur at the points of $x/R_0=-1$, $f=2.7$, $|W/W_0|=2.05$ (figure 10*b*) and $x/R_0=1.3$, $f=2.4$, $|W/W_0|=1.77$ (figure 10*d*). If the frequency of the incident wave is larger than a critical value, the amplitudes of the motion become smoother and smoother with the increase of frequency. The mechanism is that the structure loses sensitivity to external loading at high frequency. In comparison with the results of Lee *et al.* (1999), we find that the amplification of the ground motion by the subsurface crack is 73% smaller than the subsurface cavity.

8. Conclusions

In this paper, we have developed a novel method for deriving the analytical expressions of the ground motion of a half space with a semi-cylindrical canyon and beeline crack. Green's function for the half space with only a semi-cylindrical canyon was firstly obtained. The crack was then constructed by applying a series of line-source forces to satisfy the traction-free condition at the crack surfaces with Green's function. Based on the solution for the scattering of the SH wave by

an elastic half space with a semi-cylindrical canyon and the Green's function we derived, the analytical expressions of the total displacement field in the half space were obtained. This powerful methodology can be used for further studies with other topographies, such as a half space with multiple cracks and irregular canyons or hills.

We have shown that the presence of the subsurface beeline crack results in amplification of the amplitudes of the ground motion. In comparison with the no-crack condition, the crack amplifies the amplitudes of motion at all positions on the ground's surface at low frequency incident waves ($\eta = 0.1$). However, at high frequencies, the amplitudes of motion at the l.h.s. ($x/R_0 \leq -1$) are not amplified and keep almost the same magnitude as those without a crack. By contrast, the amplitudes of the r.h.s. ($x/R_0 \geq -1$) are significantly amplified. Our results also show that the amplitudes of motion are obviously amplified as the crack size increases, especially in the region on the r.h.s. of the rim C (figures 4 and 6). The positions of the crack can also have an important influence on the ground motion. Along with the continuous increase of the distance between the centre of the crack and the origin of the coordinates, the amplitudes of motion will decrease until this distance reaches up to 100 times larger than the size of the crack. In comparison with a subsurface cavity (Lee *et al.* 1999), the existence of a subsurface crack has less influence on the ground motion.

This work is supported by the National Natural Science Foundation of China through grant nos. 10628205, 10732050 and 10502031, the National Basic Research Program of China through grant no. 2004CB619304, and the SRF for ROCS, SEM. The authors are also grateful to the two anonymous reviewers for their helpful comments that have improved the manuscript significantly.

References

Aki, K. & Larner, K. L. 1970 Surface motion of layered medium having an irregular interface due to incident plane SH waves. *J. Geophys. Res.* **75**, 933–954. (doi:10.1029/JB075i005p00933)

Aki, K. & Richards, P. G. 1980 *Quantitative seismology: theory and methods.* San Francisco, CA: W. H. Freeman.

Bouchon, M. 2003 A review of the discrete wave number method. *Pure Appl. Geophys.* **160**, 445–465. (doi:10.1007/PL00012545)

Campillo, M. & Bouchon, M. 1985 Synthetic SH seismograms in a laterally varying medium by discrete wavenumber method. *Geophys. J. R. Astron. Soc.* **83**, 307–317.

Cao, J., Ge, Z. X., Zhang, J. & Chen, X. 2004 Studies on seismic waves in multi-layered media with irregular interfaces, part 1. Irregular topography problem. *Chin. J. Geophys.* **47**, 495–503.

Chen, X. 1999 Love waves in multi-layered media with irregular interfaces, I. Modal solution and excitation formulation. *Bull. Seismol. Soc. Am.* **89**, 1519–1534.

Lee, V. W. 1977 On deformations near circular underground cavity subjected to incident plane SH waves. In *Proc. Symp. of Applications of Computer Methods in Engineering, University of South CA*, pp. 951–961.

Lee, V. W. & Trifunac, M. D. 1979 Responses of tunnels to incident SH waves. *J. Eng. Mech.* **105**, 643–659.

Lee, V. W., Chen, S. & Hsu, I. R. 1999 Antiplane diffraction from canyon above subsurface unlined tunnel. *J. Eng. Mech.* **6**, 668–674. (doi:10.1061/(ASCE)0733-9399(1999)125:6(668))

Lee, V. W., Luo, H. & Liang, J. W. 2006 Antiplane (SH) waves diffraction by a semicircular cylindrical hill revisited: an improved analytic wave series solution. *J. Eng. Mech.* **10**, 1106–1114. (doi:10.1061/(ASCE)0733-9399(2006)132:10(1106))

Liu, D. K. & Han, F. 1991 Scattering of plane SH-wave on a cylindrical canyon of arbitrary shape. *Int. J. Soil Dyn. Earthquake Eng.* **10**, 249–255. (doi:10.1016/0267-7261(91)90018-U)

Liu, G. & Liu, D. K. 2007 The ground motion of an isosceles triangular hill above a subsurface cavity with incident SH waves. *Acta Mech. Solida Sin.* **28**, 60–66.

Liu, D. K. & Wang, G. Q. 2006 Antiplane SH-deformation of a semi-cylindrical hill above a subsurface cavity. *Chin. J. Theor. Appl. Mech.* **38**, 209–218.

Liu, D. K., Gai, B. Z. & Tao, G. Y. 1982 Applications of the method of complex functions to dynamic stress concentrations. *Wave Motion* **4**, 293–304. (doi:10.1016/0165-2125(82)90025-7)

Pao, Y. H. & Mow, C. C. 1973 *Diffraction and elastic waves and dynamic stress concentrations,* pp. 114–304. New York, NY: Crane, Russak & Company, Inc.

Todorovska, M. I., Hayir, A. & Trifunac, M. D. 2001 Antiplane response of a dike on flexible embedded foundation to incident SH-waves. *Soil Dyn. Earthquake Eng.* **21**, 593–601. (doi:10.1016/S0267-7261(01)00036-7)

Trifunac, M. D. 1973 Scattering of plane SH waves by a semi-cylindrical canyon. *Int. J. Earthquake Eng. Struct. Dyn.* **1**, 267–281. (doi:10.1002/eqe.4290010307)

Wong, H. L. & Trifunac, M. D. 1974 Scattering of plane SH waves by a semi-elliptical canyon. *Int. J. Earthquake Eng. Struct. Dyn.* **3**, 159–169.

Yokoi, T. & Sánchez-Sesma, F. J. 1998 A hybrid calculation technique of the indirect boundary element method and the analytical solutions for three-dimensional problems of topography. *Geophys. J. Int.* **133**, 121–139. (doi:10.1046/j.1365-246X.1998.1331466.x)

Zhang, L. & Chopra, A. K. 1991 Three-dimensional analysis of spatially varying ground motions around a uniform canyon in a homogeneous half space. *Earthquake Eng. Struct. Dyn.* **20**, 911–926. (doi:10.1002/eqe.4290201003)

Zhou, H. & Chen, X. F. 2006 A new approach to simulate scattering of SH waves by an irregular topography. *Geophys. J. Int.* **164**, 449–459. (doi:10.1111/j.1365-246X.2005.02670.x)